# Synthesis of Controllers for Exact Entrainment to Natural Oscillation*

Lijun Zhu and Zhiyong Chen
*School of Electrical Engineering and Computer Science*
*The University of Newcastle*
*Callaghan, NSW 2308, Australia*
*c3104718@uon.edu.au, zhiyong.chen@newcastle.edu.au*

Tetsuya Iwasaki
*Department of Mechanical and Aerospace Engineering*
*University of California*
*Los Angeles, CA 90095, USA*
*tiwasaki@ucla.edu*

***Abstract*— For a biologically inspired mechanical system consisting of multiple segments, its natural oscillation is defined as a periodic body movement pattern conforming to the dynamics inherent to the body-environment interaction, leading to an effective locomotion of the system. In the literature, a central pattern generator based controller has been designed to *approximately* achieve entrainment to a natural oscillation. This paper further refines the previous result by proposing a controller that achieves *exact* entrainment, as well as a rigorous stability analysis which leads to a complete solution to the problem of entrainment to natural oscillation.**

***Index Terms*— Oscillator, limit cycle, central pattern generator (CPG), locomotion**

## I. Introduction

It is believed that fundamental locomotion control principles designed by nature are hidden in various animal behaviors including swimming, crawling, flying, walking, etc. The principles are of particular interest to control engineers as they enable designs of highly intelligent and efficient mechanical machines with robustness, adaptivity, and autonomy. Biologists discovered that the energy consumption during locomotion is minimized by exploiting the body movement pattern [1], [2]. The results reported in this paper are part of a larger effort to find an engineering analogue of this discovery, investigating an appropriate movement pattern, called natural oscillation, as well as the corresponding control principles.

To facilitate the research, we focus on a class of multi-link systems mimicking animal locomotion behaviors such as snake crawling or eel swimming. The system is a chain of multiple links connected through rotational joints, placed on a horizontal plane. This is a typical rectifier system [3] which, under certain coordinated oscillations of the inputs (rhythmic body movements), produces biased outputs (forward velocities). Essentially, the locomotion of this system consists of two components, the undulatory body movement and the effect of rectification. The body movement in an optimal pattern in a certain sense is expected to be rectified to generate an effective translation of the whole body. We conjecture that an optimally efficient pattern can be characterized as a natural oscillation of the body-environment system. In particular, a natural mode of oscillation is defined in [4] to be a free response of the modified system obtained by properly reducing the damping effects to achieve marginal stability for sustained oscillations.

Once a natural oscillation is properly defined, the following task is to find the control principle for actuating the system body to realize the natural oscillation in a stable manner via feedback. Biological control mechanisms for animal locomotion are known to consist of neuronal circuits, called the central pattern generator (CPG) [5]–[7]. A CPG can be modeled as a nonlinear oscillator, and when placed in a feedback loop, provides a basic control architecture to achieve coordinated oscillations of engineered systems [8]–[10]. Within the CPG framework, feedback control laws to achieve entrainment to a resonance have been studied for one degree-of-freedom (DOF) systems [11]–[16] as well as for multi-DOF standard mechanical systems (which are described by symmetric positive definite mass, stiffness, and damping matrices) [17], [18].

Recently, we showed [4] how a CPG based controller can be designed to achieve the natural oscillation for non-standard mechanical systems with asymmetric stiffness matrix, arising from dynamics of animal locomotion. Technically, the development in [4] is within the framework of multivariable harmonic balance (MHB) [19], [20]. The MHB approach is used to characterize the design specification approximately, and systematic methods are proposed to find the controller parameters that satisfy the MHB condition exactly. Though MHB equations characterize the design specification effectively and simply, yet it is at the expense of losing accuracy. Moreover, the asymptotic stability of the closed-loop system is not theoretically guaranteed but demonstrated only by numerical simulation. To overcome the two disadvantages in the MHB based controller, this paper will further investigate an exact controller with a rigorous stability analysis.

The remaining sections are organized as follows. The definition of natural oscillation will be revisited in Section II followed by the precise formulation for the problem of

*This work is partially supported by Australian Research Council Grant DP0878724 to Z. Chen and by NSF No.0654070 and ONR MURI Grant N00014-08-1-0642 to T. Iwasaki.

exact entrainment to natural oscillation. The main result and its proof are given in Section III. A numerical example is given in Section IV to illustrate the effectiveness of the exact controller. Finally, the paper is closed in Section V. Throughout this paper, $\Re(x)$ and $\Im(x)$ represent the real and imaginary parts of $x$, respectively.

## II. Problem Formulation

The locomotion of a class of mechanical systems, e.g., snake-like multi-link systems, is achieved by the coordinated oscillations of the body segments. The mechanical dynamics act as a rectifier that converts the undulatory body movement into a forward velocity. We are interested in a special oscillation pattern, called natural oscillation, which may naturally lead to an appropriate forward locomotion. More specifically, the oscillation dynamics can be characterized by a linearized model as follows (see [4])

$$J\ddot{\theta} + \mu J\dot{\theta} + K\theta = u, \quad K = K_o + v\Lambda \tag{1}$$

where $\theta \in \mathbb{R}^n$ represents the shape variables for the body, e.g., the link angles. The matrices $J, K \in \mathbb{R}^{n\times n}$ are the inertia and stiffness matrices respectively, $\mu \in \mathbb{R}$ is the environmental force constant and $u \in \mathbb{R}^n$ is the controller input vector representing the joint torques. Note that the stiffness matrix $K$ is not necessarily symmetric, where $K_o$ is a symmetric positive definite matrix representing the body stiffness, and $v\Lambda$ is an asymmetric matrix representing the skewed stiffness arising from locomotion at a velocity $v \in \mathbb{R}$ relative to the environment. In (1), we impose the following:

**Assumption 1:**

(a) $J, K \in \mathbb{R}^{n\times n}$ and $J = J^{\mathsf{T}} > 0$.

(b) All the eigenvalues of $M := J^{-1}K$ are simple and have positive real parts.

In [4], the natural oscillation is defined as a free response of the modified system obtained by reducing the damping effect to achieve marginal stability for sustained oscillations. The definition is given below.

**Definition 2.1:** (Natural Oscillation) Consider the system described by (1) with Assumption 1. Let the damping effect be adjusted by a parameter $\epsilon \in \mathbb{R}$ and define the modified system with no input:

$$J\ddot{\theta} + (\mu - \epsilon)J\dot{\theta} + K\theta = 0. \tag{2}$$

Suppose that there exists a value of $\epsilon$ such that the system is marginally stable with a single pair of complex eigenvalues on the imaginary axis. Let such value of $\epsilon$ be denoted by $\varrho$, and the eigenvalues and eigenvector be $\pm j\omega$ and $z$, respectively. Then, the resulting periodic trajectory $\theta(t) = \Re[ze^{j\omega t}]$ of (2) is called the *natural oscillation* $(\omega, z)$ of the original system (1), where $\varrho$, $\omega$ and $z$ are referred to as the *damping factor, natural frequency*, and *mode shape* of the natural oscillation, respectively.

The natural oscillation can be explicitly calculated from the spectral decomposition. Let $\mathbb{M}$ be the set of eigenvalue, eigenvector, and left eigenvector of $M$:

$$\begin{aligned}\mathbb{M} := \{(\alpha, \zeta, l) \in \mathbb{C}\times\mathbb{C}^n\times\mathbb{C}^n :\\ (\alpha I - M)\zeta = 0,\ l^*(\alpha I - M) = 0,\ l^*\zeta = 1\ \},\end{aligned}$$

where the superscript $^*$ is the conjugate transpose operator. The following lemma [4] characterizes the natural oscillation.

**Lemma 2.1:** *Consider the system in (1) with Assumption 1. Let*

$$\varrho := \min_{(\alpha,\zeta,l)\in\mathbb{M}} \quad \mu + \frac{\Im(\alpha)}{\sqrt{\Re(\alpha)}} \tag{3}$$

*and suppose the minimizer is unique and is denoted by $(\varsigma, z, \ell)$. Then, the natural oscillation of (1) is given by $(\omega, z)$ with damping factor $\varrho$ where $\omega := \sqrt{\Re(\varsigma)}$.*

To realize the natural oscillation $(w, z)$ for the mechanical system (1), the simplest approach is to exactly cancel the damping factor by implementing a controller $u = \varrho J\dot{\theta}$ with a properly selected initial condition. Obviously, this approach is not practical because it is critically sensitive to the parameter $\varrho$ and the initial condition. In fact, it is the main objective of this paper to propose a practically implementable controller to achieve the exact entrainment to a natural oscillation with structural stability.

**Definition 2.2:** (Exact Entrainment) For the system (1), consider a feedback controller of the form $u = g(\theta, \dot{\theta})$. Let the orbit of the natural oscillation $(\omega, z)$ be defined by

$$\begin{aligned}&\mathbb{O} := \{\ (\vartheta(t), \dot{\vartheta}(t)) \in \mathbb{R}^n\times\mathbb{R}^n \mid t\in\mathbb{R}\ \},\\ &\vartheta(t) := Z\sin(\omega t + \phi), \quad Ze^{j\phi} := z,\end{aligned}$$

where $Z$ is the diagonal matrix with entries $|z_i|$ and $\phi$ is a vector with entries $\angle z_i$. A controller is said to achieve exact entrainment to the natural oscillation $(\omega, z)$ if the following property holds: When the initial condition $(\theta(0), \dot{\theta}(0))$ is sufficiently close to the orbit $\mathbb{O}$, i.e., when

$$\min_{(\vartheta_o,\dot{\vartheta}_o)\in\mathbb{O}} \|\theta(0) - \vartheta_o\| + \|\dot{\theta}(0) - \dot{\vartheta}_o\|$$

is sufficiently small, the trajectory of the closed-loop system $\theta(t)$ converges to the orbit $\mathbb{O}$, i.e., there exists $t_o$, dependent upon the initial condition, such that

$$\lim_{t\to\infty} \theta(t) - \vartheta(t + t_o) = 0.$$

Inspired by CPG control mechanisms in animal locomotion, some nonlinear controllers have been constructed in [4] for the problem of entrainment to natural oscillation. A typical positive rate feedback controller is given in the form:

$$u = \epsilon J\dot{\theta} + rJZ\psi(q), \ q = \eta Z^{-1}\dot{\theta} \tag{4}$$

where $\psi$ is some nonlinear function. However, the insufficiency of the controller given in [4] is two fold. First, the trajectory $\theta(t)$ of the closed-loop system converges to the desired $\vartheta(t)$ only in the approximate sense where the higher order harmonic terms of $\theta(t)$ are ignored. In particular, in the harmonic balance analysis, the nonlinear term is approximated as $\psi(x) \approx \kappa(a)x$ for $x(t) = a\sin(\omega t)$, where $\kappa$ is the describing function of $\psi$. Secondly, numerical simulation shows that the asymptotic trajectory of the closed-loop is a stable limit cycle, but it lacks a rigorous stability analysis. It has been proven that once $\psi(q)$ is quasi-linearized at the desired trajectory $\vartheta(t)$, the resulting linear system is marginally stale, which hence induces an natural oscillation $\vartheta(t)$. However, it is important to know whether $\vartheta(t)$ is a stable limit cycle of the original nonlinear system. Once $\theta(t)$ is deviated from $\vartheta(t)$, it should be asymptotically attracted to $\vartheta(t)$, but this property has yet to be well addressed.

## III. MAIN RESULTS

We will propose a controller in the form of (4) by appropriately choosing the nonlinear function such that the exact entrainment of $\theta(t)$ to $\vartheta(t)$ can be achieved with a rigorous proof for stability. The main result of this paper is now stated.

**Theorem 3.1:** *Consider the system (1) with Assumption 1. Let $(\omega, z)$ be the natural oscillation with damping factor $\varrho$ as described in Lemma 2.1. Let $\eta, \epsilon \in \mathbb{R}$ be such that $\eta > 0$, $\epsilon < \varrho$, and let $\kappa(x)$ be a function that is continuously differentiable, strictly decreasing, and positive on $x > 0$. Then, the controller (4) with*

$$r = (\varrho - \epsilon)/(\kappa(\eta\omega)\eta), \quad \psi(q) = \kappa(\|R^\dagger Z q\|)q$$

*achieves the exact entrainment to the natural oscillation $(\omega, z)$, where $Z$ is the diagonal matrix with entries $|z_i|$, and*

$$R = \left[\begin{array}{cc} \Im(z) & \Re(z) \end{array}\right], \; R^\dagger = 2\left[\begin{array}{cc} \Im(\ell) & \Re(\ell) \end{array}\right]^\mathsf{T}.$$

*Proof:* For convenience of proof, we first define some notation. It is easy to show that

$$\left[\begin{array}{cc} z & z^* \end{array}\right]\Gamma^{-1} = R, \quad \Gamma\left[\begin{array}{c} \ell^* \\ \ell^\mathsf{T} \end{array}\right] = R^\dagger, \quad \Gamma := \left[\begin{array}{cc} j & -j \\ 1 & 1 \end{array}\right]$$

and hence

$$R^\dagger R = \Gamma\left[\begin{array}{c} \ell^* \\ \ell^\mathsf{T} \end{array}\right]\left[\begin{array}{cc} z & z^* \end{array}\right]\Gamma^{-1} = I.$$

That is, $R^\dagger$ is a pseudo-inverse of $R$. Let matrices $N \in \mathbb{R}^{n\times(n-2)}$ and $N^\dagger \in \mathbb{R}^{(n-2)\times n}$ be such that

$$N^\dagger N = I, \; R^\dagger N = 0, \; N^\dagger R = 0.$$

Such matrices exist due to the assumption that the eigenvalues of $M$ are simple. In particular, the columns of $N$ (row of $N^\dagger$) can be the real and imaginary parts of the $(n-2)$ right (left) eigenvectors of $M$ corresponding to the eigenvalues other than $\varsigma$ or $\varsigma^*$. Some simple calculation gives

$$R^\dagger M R = \left[\begin{array}{cc} a & -b \\ b & a \end{array}\right], \; a = \Re(\varsigma), \; b = \Im(\varsigma),$$
$$R^\dagger M N = 0, \; N^\dagger M R = 0.$$

Finally, we define a nonsingular matrix $T$ as follows:

$$T := \left[\begin{array}{c} R^\dagger \\ N^\dagger \end{array}\right], \quad T^{-1} = \left[\begin{array}{cc} R & N \end{array}\right].$$

The closed-loop system under consideration is

$$\ddot{\theta} + (\mu - \epsilon - r\eta\kappa(\|R^\dagger\eta\dot{\theta}\|))\dot{\theta} + M\theta = 0. \tag{5}$$

Under the new coordinate

$$\wp := \left[\begin{array}{c} \wp_1 \\ \wp_2 \end{array}\right] := T\theta, \; \wp_1 \in \mathbb{R}^2, \; \wp_2 \in \mathbb{R}^{n-2},$$

the closed-loop system (5) becomes

$$\ddot{\wp}_1 + (\mu - \epsilon - r\eta\kappa(\|\eta\dot{\wp}_1\|))\dot{\wp}_1 + R^\dagger M R\wp_1 = 0 \tag{6}$$
$$\ddot{\wp}_2 + (\mu - \epsilon - r\eta\kappa(\|\eta\dot{\wp}_1\|))\dot{\wp}_2 + N^\dagger M N\wp_2 = 0. \tag{7}$$

In what follows, we will investigate these two subsystems (6) and (7), respectively.

For the upper subsystem (6), we write $\wp_1$ in the polar coordinate:

$$\wp_1 = \xi\left[\begin{array}{c} \cos\varpi \\ \sin\varpi \end{array}\right]$$

with the radius $\xi \in \mathbb{R}$ and the angle $\varpi \in \mathbb{R}$. For convenience, we define two vectors

$$v_1 = \left[\begin{array}{c} \cos\varpi \\ \sin\varpi \end{array}\right], \; v_2 = \left[\begin{array}{c} -\sin\varpi \\ \cos\varpi \end{array}\right].$$

Then we have

$$\dot{\wp}_1 \;=\; \dot{\xi}v_1 + \xi v_2\dot{\varpi}$$

and hence, together with (6),

$$\begin{aligned} \ddot{\wp}_1 &= \ddot{\xi}v_1 + \dot{\xi}v_2\dot{\varpi} + \dot{\xi}v_2\dot{\varpi} - \xi v_1\dot{\varpi}^2 + \xi v_2\ddot{\varpi} \\ &= -(\mu - \epsilon - r\eta\kappa(\|\eta\dot{\wp}_1\|))(\dot{\xi}v_1 + \xi v_2\dot{\varpi}) \\ &\quad -R^\dagger M R\xi v_1. \end{aligned}$$

Multiplying $v_1^\mathsf{T}$ and $v_2^\mathsf{T}$ from left on the above equation gives the following two equations, (noting $v_1^\mathsf{T}v_2 = v_2^\mathsf{T}v_1 = 0$ and $v_1^\mathsf{T}v_1 = v_2^\mathsf{T}v_2 = 1$)

$$\ddot{\xi} - (b/\omega)\dot{\xi} - r\eta\delta\dot{\xi} + \xi(\omega^2 - \dot{\varpi}^2) = 0$$
$$\ddot{\varpi} + 2(\dot{\xi}/\xi)\dot{\varpi} - (b/\omega)(\dot{\varpi} - \omega) - r\eta\delta\dot{\varpi} = 0. \tag{8}$$

where $\delta := \kappa(\|\eta\dot{\wp}_1\|) - \kappa(\eta\omega)$ and the following facts are used:

$$v_1^\mathsf{T}R^\dagger M R v_1 = a = \omega^2, \; v_2^\mathsf{T}R^\dagger M R v_1 = b,$$
$$\mu - \epsilon - r\eta\kappa(\eta\omega) = -b/\omega.$$

We consider the system (8) as a three dimensional system with states $(\xi, \dot{\xi}, \dot{\varpi})$. Obviously, the system has an equilibrium point $(\xi, \dot{\xi}, \dot{\varpi}) = (1, 0, \omega)$. Next, we will show this equilibrium point is asymptotically stable. To this end, we define $(\bar{\xi}, \dot{\bar{\xi}}, \dot{\bar{\varpi}}) = (\xi - 1, \dot{\xi}, \dot{\varpi} - \omega)$ and the linearized system at $(\bar{\xi}, \dot{\bar{\xi}}, \dot{\bar{\varpi}}) = (0, 0, 0)$ is

$$\begin{aligned} \ddot{\bar{\xi}} - g_1 \dot{\bar{\xi}} - 2\dot{\bar{\varpi}}\omega = 0 \\ \ddot{\bar{\varpi}} + 2\omega\dot{\bar{\xi}} - g_1\dot{\bar{\varpi}} - g_2(\omega^2\bar{\xi} + \omega\dot{\bar{\varpi}}) = 0 \end{aligned} \tag{9}$$

where $g_1 = b/\omega < 0, \;\; g_2 := r\eta^2\kappa'(\eta\omega) < 0$ and

$$\begin{aligned} \delta &= \kappa(\|\eta\dot{\wp}_1\|) - \kappa(\eta\omega) \approx (\eta/\omega)\kappa'(\eta\omega)\dot{\wp}_1^{\intercal}(\dot{\wp}_1 - v_2\omega) \\ &= (\eta/\omega)\kappa'(\eta\omega)(\dot{\xi}v_1 + \xi v_2\dot{\varpi})^{\intercal}(\dot{\xi}v_1 + \xi v_2\dot{\varpi} - v_2\omega) \\ &\approx \eta\kappa'(\eta\omega)(\bar{\xi}\omega + \dot{\bar{\varpi}}). \end{aligned}$$

The characteristic equation for (9) is

$$a_3 s^3 + a_2 s^2 + a_1 s + a_0 = 0$$

with $a_3 = 1$, $a_2 = -(2g_1 + g_2\omega) > 0$, $a_1 = g_1^2 + g_1 g_2\omega + 4\omega^2$, and $a_0 = -2g_2\omega^3 > 0$. We can use the Routh table to verify that all the roots are in the open left half plane, and thus conclude stability of (9). In other words, we have $\lim_{t\to\infty}\xi(t) = 1$ and $\lim_{t\to\infty}\dot{\bar{\varpi}}(t) = 0$ exponentially. The latter implies

$$\lim_{t\to\infty}\int_0^t \dot{\bar{\varpi}}(\tau)d\tau$$

exists, or equivalently, there exists a constant

$$\varpi_o := \lim_{t\to\infty}\Big(\varpi(t) - \omega t\Big).$$

As a result, we have

$$\lim_{t\to\infty}\wp_1(t) - \begin{bmatrix}\cos(\omega t + \varpi_o) \\ \sin(\omega t + \varpi_o)\end{bmatrix} = 0.$$

With $\xi = 1$ and $\varpi(t) = \omega t + \varpi_o$, the lower subsystem (7) becomes

$$\ddot{\wp}_2 - (b/\omega)\dot{\wp}_2 + N^{\dagger}MN\wp_2 = 0$$

which has the following characteristic equation

$$\det(\lambda^2 I - (b/\omega)\lambda I + N^{\dagger}MN) = 0. \tag{10}$$

Let $\mathbb{A}$ be the set of eigenvalues of $M$ other than $\varsigma$ and $\varsigma^*$. Because $N$ is spanned by the $n-2$ eigenvectors of $M$ associated with $\mathbb{A}$, for each eigenvalue $\alpha \in \mathbb{A}$, there exists a vector $w$ such that $M(Nw) = \alpha(Nw)$, and hence, $N^{\dagger}MNw = \alpha N^{\dagger}Nw = \alpha w$. Thus, $\mathbb{A}$ coincides with the set of eigenvalues of $N^{\dagger}MN$. Accordingly, $\lambda$ is a characteristic root of equation (10) if and only if it satisfies

$$\lambda^2 - (b/\omega)\lambda + \alpha = 0$$

for some $\alpha \in \mathbb{A}$. From Lemma 5.1 in the appendix, the polynomial is Hurwitz since $\varsigma$ is given by (3) and $b/\omega = \Im(\varsigma)/\sqrt{\Re(\varsigma)}$. As a result, we have $\lim_{t\to\infty}\wp_2(t) = 0$.

Let

$$\vartheta(t) = R\begin{bmatrix}\cos(\omega t) \\ \sin(\omega t)\end{bmatrix} = Z\sin(\omega t + \phi), \; t_o = \varpi_o/\omega.$$

It now follows that

$$\begin{aligned} &\lim_{t\to\infty}\theta(t) - \vartheta(t + t_o) = \lim_{t\to\infty}T^{-1}\wp(t) - \vartheta(t + t_o) \\ &= \lim_{t\to\infty}R\wp_1(t) + N\wp_2(t) - R\begin{bmatrix}\cos(\omega t + \varpi_o) \\ \sin(\omega t + \varpi_o)\end{bmatrix} = 0. \end{aligned}$$

The proof is thus complete. ■

## IV. Numerical Example

The model (1) captures the locomotion behavior for a multi-link system interacting with environment. A typical example, called a fliptail system, is given in [4], [21]. When the tail of the system flaps in a certain pattern, the friction force between body and environment drives it forward. Contrarily, if the system is pulled forward with a constant velocity $v$, its segmental body is expected to oscillate in a natural pattern. The dynamic model of this scenario is in the form of (1) with the matrices $J$ and $K$ given by

$$\begin{aligned} &J = m_o l_o^2(FF^{\intercal} + I/3), \; \mu = \mu_n/m_o, \; K = v\Lambda + k_o BB^{\intercal}, \\ &\Lambda = (\mu_n - \mu_t)l_o F + \mu_t l_o \text{diag}(Fe), \end{aligned}$$

where

$$F = \begin{bmatrix} 1 & -1 & & \\ & \ddots & \ddots & \\ & & 1 & -1 \\ & & & 1 \end{bmatrix}, \; B = \begin{bmatrix} 1 & 2 & \cdots & 2 \\ & 1 & \ddots & \vdots \\ & & \ddots & 2 \\ & & & 1 \end{bmatrix}$$

and $e \in \mathbb{R}^n$ is the vector with all its entries being one. In the simulations, we use the following parameter values: The number of links for the tail is $n = 5$, and each link has mass $m_o := m/n$ and length $2l_o = l/n$, where the total length is $l = 0.5$ m and mass is $m = 0.2$ kg. The environmental force constants are $\mu_t = 0$ and $\mu_n = 0.2$ Ns/m, and each joint has stiffness $k_o = 1.25 \times 10^{-3}$ Nm/rad. The nonlinear function $\kappa$ in Theorem 3.1 is chosen as $\kappa(x) = 1/(1 + x)$.

First, the natural oscillation has been found as in Table I.[1] Two pairs of controller parameters, $(\eta, \epsilon) = (2, 2.3)$ and $(\eta, \epsilon) = (3, 0)$ are used in the simulations. The profile of the natural oscillation with a positive differential feedback (PDF) controller [4] is given in Table II. We note that the natural oscillation can be achieved approximately.

Next, to obtain an exact solution, we apply the controller developed in Theorem 3.1. For the two pairs of parameters $(\eta, \epsilon) = (2, 2.3)$ and $(\eta, \epsilon) = (3, 0)$, the performance of exact entrainment to the natural oscillation is shown in Table III.

Finally, the waveforms of the oscillations with the PDF controller and the exact controller are given in Figures 1 and 2. As expected, it can be seen that the approximate natural oscillation deviates from sinusoidal waveforms, but the exact one does not.

[1] In the tables, without loss of generality, we set $\phi_5 = 0°$ to be the reference phase, and $a_i$ is the amplitude of $\theta_i(t)$.

TABLE I

PROFILE OF THE NATURAL OSCILLATION

| Period | $\phi_1$ | $\phi_2$ | $\phi_3$ | $\phi_4$ |
|---|---|---|---|---|
| 1.97 | 183.6° | 121.6° | 76.5° | 20.2° |

| $a_1$ | $a_2$ | $a_3$ | $a_4$ | $a_5$ |
|---|---|---|---|---|
| 2.4° | 8.9° | 16.1° | 29.2° | 45.6° |

TABLE II

PROFILE OF THE OSCILLATION WITH A PDF CONTROLLER

| $\eta$, $\epsilon$ | Period | $\phi_1$ | $\phi_2$ | $\phi_3$ | $\phi_4$ |
|---|---|---|---|---|---|
| 2, 2.3 | 1.97 | 183.1° | 120.9° | 75.7° | 19.5° |
| 3, 0 | 1.99 | 186.1° | 120.3° | 75.6° | 17.6° |

| $\eta$, $\epsilon$ | $a_1$ | $a_2$ | $a_3$ | $a_4$ | $a_5$ |
|---|---|---|---|---|---|
| 2, 2.3 | 2.4° | 8.9° | 16.1° | 29.3° | 45.9° |
| 3, 0 | 2.4° | 9.2° | 17.2° | 30.9° | 50.4° |

TABLE III

PROFILE OF THE OSCILLATION WITH AN EXACT CONTROLLER

| $\eta$, $\epsilon$ | Period | $\phi_1$ | $\phi_2$ | $\phi_3$ | $\phi_4$ |
|---|---|---|---|---|---|
| 2, 2.3 | 1.97 | 183.6° | 121.6° | 76.5° | 20.2° |
| 3, 0 | 1.97 | 183.6° | 121.6° | 76.5° | 20.2° |

| $\eta$, $\epsilon$ | $a_1$ | $a_2$ | $a_3$ | $a_4$ | $a_5$ |
|---|---|---|---|---|---|
| 2, 2.3 | 2.4° | 8.9° | 16.1° | 29.2° | 45.6° |
| 3, 0 | 2.4° | 8.9° | 16.1° | 29.2° | 45.6° |

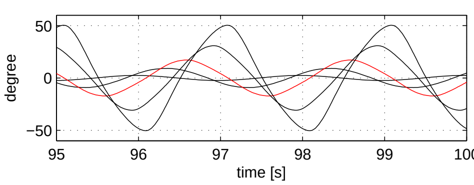


Fig. 1. Non-sinusoidal trajectories of the closed-loop system with PDF controller.

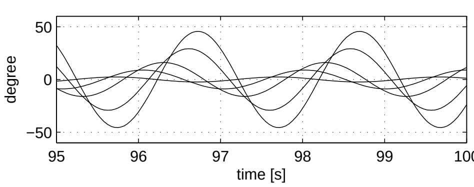


Fig. 2. Sinusoidal trajectories of the closed-loop system with exact controller.

## V. CONCLUSION

In this paper, we have considered the exact entrainment controller inspired by the CPG control principle, which is applied to achieve the natural oscillation of the mechanical systems arising from typical dynamics of animal locomotion. The natural oscillation is sinusoidal and it is a limit cycle of the system. We have proven that if the nonlinear function adopted by the controller has a negative slope, then the limit cycle is locally asymptotically stable. In other words, the system trajectories in the neighborhood of the limit cycle always converge to it and the exact entrainment to natural oscillation is thus achieved.

## APPENDIX

**Lemma 5.1:** *For any $\varsigma \in \mathbb{C}$ with $\Re(\varsigma) > 0$, the polynomial*

$$p(\varsigma, \lambda) := \lambda^2 + a\lambda + \varsigma = 0, \tag{11}$$

*is Hurwitz (i.e., the solution $\lambda$ has negative real part,) if and only if $a > |\Im(\varsigma)|/\sqrt{\Re(\varsigma)}$.*

*Proof:* The polynomial $p(\varsigma, \lambda)$ is Hurwitz if and only if the polynomial with real coefficients $q(\lambda) := p(\varsigma, \lambda)p(\varsigma^*, \lambda)$ is Hurwitz. It is straightforward to verify using the Routh stability criterion that $q(\lambda)$ is Hurwitz if and only if $a > |\Im(\varsigma)|/\sqrt{\Re(\varsigma)}$. ■

## REFERENCES


[1] G.A. Cavagna, N.C. Heglund, and C.R. Taylor. Mechanical work in terrestrial locomotion: Two basic mechanisms for minimizing energy expenditure. *Am. J. Physiol.*, 233:R243–R261, 1977.

[2] J. Rose and J.G. Gamble. *Human Walking*. Lippincott Williams and Wilkins, 2003.

[3] J. Blair and T. Iwasaki. Optimal gaits for mechanical rectifier systems. *IEEE Trans. Auto. Contr.*, 2010. (To appear).

[4] Z. Chen and T. Iwasaki. Matrix perturbation analysis for weakly coupled oscillators. *Systems & Control Letters*, 58(2):148–154, 2009. (DOI:10.1016/j.sysconle.2008.10.002).

[5] T.G. Brown. The intrinsic factors in the act of progression in the mammal. *Proc. Roy. Soc. Lond.*, 84:308–319, 1911.

[6] S. Grillner, J.T. Buchanan, P. Walker, and L. Brodin. *Neural Control of Rhythmic Movements in Vertebrates*. New York: Wiley, 1988.

[7] G.N. Orlovsky, T.G. Deliagina, and S. Grillner. *Neuronal Control of Locomotion: From Mollusc to Man*. Oxford University Press, 1999.

[8] Y. Fukuoka, H. Kimura, and A.H. Cohen. Adaptive dynamic walking of a quadruped robot on irregular terrain based on biological concepts. *Int. J. Robotics Research*, 22(3-4):187–202, 2003.

[9] G. Taga. Self-organized control of bipedal locomotion by neural oscillators in unpredictable environment. *Biol. Cybern.*, 65:147–159, 1991.

[10] M.A. Lewis and G.A. Bekey. Gait adaptation in a quadruped robot. *Autonomous Robots*, 12(3):301–312, 2002.

[11] N.G. Hatsopoulos. Coupling the neural and physical dynamics in rhythmic movements. *Neural Computation*, 8(3):567–581, 1996.

[12] M.M. Williamson. Neural control of rhythmic arm movements. *Neural Networks*, 11:1379–1394, 1998.

[13] B.W. Verdaasdonk, H.F. Koopman, and F.C. Van der Helm. Energy efficient and robust rhythmic limb movement by central pattern generators. *Neural Network*, 19(4):388–400, 2006.

[14] B.W. Verdaasdonk, H.F. Koopman, and F.C. Van der Helm. Resonance tuning in a neuro-musculo-skeletal model of the forearm. *Biological Cybernetics*, 96(2):165–180, 2007.

[15] T. Iwasaki and M. Zheng. Sensory feedback mechanism underlying entrainment of central pattern generator to mechanical resonance. *Biological Cybernetics*, 94(4):245–261, 2006.

[16] Y. Futakata and T. Iwasaki. Formal analysis of resonance entrainment by central pattern generator. *J. Math. Biol.*, 57(2):183–207, 2008.

[17] Y. Futakata and T. Iwasaki. Entrainment of central pattern generators to natural oscillations of collocated mechanical systems. *IEEE Conf. Decision and Contr.*, 2008.

[18] Y. Futakata. Natural mode entrainment by CPG-based decentralized feedback controllers. *Ph.D Dissertation, Mechanical and Aerospace Engineering, University of Virginia*, August, 2009.

[19] A. Gelb and W.E.V. Velde. *Multiple-input describing functions and nonlinear system design*. McGraw-Hill, New York, 1968.

[20] T. Iwasaki. Multivariable harmonic balance for central pattern generators. *Automatica*, 44(12):4061–4069, 2008.

[21] M. Saito, M. Fukaya, and T. Iwasaki. Serpentine locomotion with robotic snake. *IEEE Control Systems Magazine*, 22(1):64–81, 2002.